RADIATION EFFECTS IN THE TRANSIENT HOT-WIRE TECHNIQUE
Measurement of the thermal conductivity of *n*-pentane

*Y. Shi, L. Sun, J. E. S. Venart and R. C. Prasad**

Department of Engineering, University of New Brunswick, Saint John, NB E2L 4L5, Canada

The transient hot-wire technique is widely used for absolute measurements of the thermal conductivity and thermal diffusivity of fluids. It is well established that fluid radiation effects significantly influence these measurements, especially those for the thermal diffusivity. Corrections for radiation effects are based on the models developed and deviations of the measured data from the ideal line source model. In this paper, the effect of fluid radiation on the measurements of the thermal conductivity of *n*-pentane is presented. For comparison, the influence of thermal radiation effect on measurement of transparent fluids, such as argon is also shown. The difference between the influence of natural convection and thermal radiation is also demonstrated.

Keywords: *argon, hot-wire technique, natural convection, n-pentane, thermal conductivity, thermal radiation*

Introduction

The transient hot-wire instrument provides rapid and accurate measurements of the fluid thermal conductivity. A series of corrections must be made to account for differences between the actual and ideal heat transfer models [1–5]. This paper summarizes the development of thermal radiation effects in order to more clearly demonstrate this influence on the measurement of the thermal conductivity of fluids. Thermal radiation effects on fluids transparent to thermal radiation are different from those for fluid which absorb thermal radiation. Both cases are discussed in this paper. The $\Delta T \sim \ln t$ plot for absorbing fluids, such as liquid *n*-pentane, as well as that for transparent fluids, such as argon is also discussed. It is necessary as well to differentiate between the influence of natural convection and thermal radiation. In this technique, natural convection is always preceded by a convection free period during which measurements are not influenced by this effect. Fluid thermal radiation, however, begins from the very beginning and its influence is observed in the initial measurement as well.

Methodology

The transient hot-wire method is widely accepted as a primary instrument for accurate measurement of fluid thermal conductivity on a wide variety of fluids. Though theoretically feasible, practical simultaneous use for thermal diffusivity measurements has been limited due to the lack of reproducibility and an apparent dependence of the results on the power employed. The instrument consists of a very thin and long wire vertically submerged in the test fluid. A constant current through the wire results in heat dissipation into the surrounding fluid and a transient temperature rise of the wire from which the thermal conductivity of the fluid can be determined. The working equation for thermal conductivity is based on the transient solution of Fourier's law for an infinite line source [4, 5]. The ideal temperature rise of the fluid, at the wire–fluid interface, $r=a$, at time t is

$$\Delta T = \frac{q}{4\pi\lambda(\rho,T)}\ln\frac{4\alpha t}{a^2 C} \tag{1}$$

where

$$\Delta T = \Delta T_{\mathrm{w}} + \sum \delta T_{\mathrm{i}}$$

and $\Sigma\delta T_{\mathrm{i}}$ are appropriate corrections to the measured temperature rise, ΔT_{w}, q is the power per unit length applied to the wire, λ is the thermal conductivity, $\alpha=\lambda/(\rho C_{\mathrm{p}})$ is the thermal diffusivity, ρ is the density, and C_{p} is the isobaric heat capacity (all for the fluid), with C=1.781… the exponential of Euler's constant. One of the necessary corrections to ΔT_{w} accounts for the effect of thermal radiation δT_{rad}.

For fluids which absorb radiation, Nieto de Castro *et al.* [6–8] have shown that the dominant correction term in the heat flux gradient arises from the emission of radiation by the heated fluid [9]. These considerations allowed them to derive an approximate analytical solution to the applicable energy equation.

* Author for correspondence: prasad@unb.ca

The temperature rise of the test fluid at the wire surface, ΔT_2, is given by [7]:

$$\Delta T_2 = \frac{q}{4\pi\lambda_2}\ln\frac{4\alpha_2 t}{a^2C}\left(1+\frac{Ba^2}{4\alpha_2}\right)-\frac{qBt}{4\pi\lambda_2}+ + \frac{qBa^2}{16\pi\lambda_2\alpha_2}+O\left(\frac{a^2}{\alpha_2 t}, B^2t^2\right) \quad (2)$$

where

$$B=\frac{16Kn^2\sigma T_0^2}{(\rho C_\mathrm{p})_2}$$

and, the correction for radiation absorbing fluids is [11]:

$$\delta T_\mathrm{rad} = -\frac{qB}{4\pi\lambda_2}\left[\frac{a^2}{4\alpha_2}\ln\left(\frac{4\alpha_2 t}{a^2C}\right)-t+\frac{a^2}{4\alpha_2}\right] \quad (3)$$

In this result, however, the wire itself was regarded as part of the fluid since the inner boundary condition was considered to be r=0 and not r=a.

To eliminate this inaccuracy, the following solution is obtained [1] using the inner boundary condition, r=a, and assuming the thermophysical properties of the wire to be constant:

$$\Delta T_1(a,t)=\Delta T_\mathrm{w}(a,t)+\frac{fa^2q\lambda_1\alpha_2}{8\pi\lambda_2^2\alpha_1}\ln\frac{4\alpha_2 t}{a^2C}+ + \frac{qfa^2}{16\pi\lambda_2}\left(\frac{-\pi^2}{6}+\ln^2\frac{4\alpha_2 t}{a^2C}\right)-\frac{qf\alpha_2 t}{4\pi\lambda_2}-\frac{qfa^2}{8\pi\lambda_2} \quad (4)$$

where

$$f=\frac{B}{\alpha_2}$$

and

$$B=\frac{16Kn^2\sigma T_0^2}{(\rho C_\mathrm{p})_2}$$

The temperature rise ΔT_w represents the corrected measured temperature difference (aside from fluid radiation) and ΔT_1 the ideal, and now radiation-corrected temperature difference. K is the mean absorption coefficient and n is the refractive index of the fluid (both considered temperature independent), σ is the Stephan–Boltzmann constant, and the subscript 1 refers to the properties of wire and subscript 2 refers to the properties of fluids.

For fluids which are transparent to thermal radiation, the radiation effect can be corrected by [5]

$$\delta T_\mathrm{rad} = \frac{8\pi a\varepsilon_\mathrm{p}\sigma T_0^3\Delta T^2}{q} \quad (5)$$

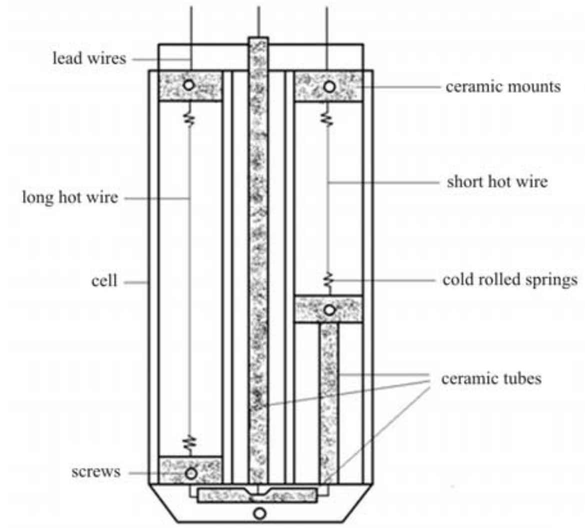

Fig. 1 Schematic diagram of the hot-wire cell

Experimental

A transient hot-wire instrument was modified to allow improved measurements of both thermal conductivity and thermal diffusivity [10–12]. Two wires of different lengths were used for end effect compensation (Fig. 1). The principle of the measurement and details of the apparatus are described elsewhere [10, 11]. The apparatus [11] includes a pressurizing system and an isothermal block to maintain the test fluid at a desired pressure (up to 70 MPa) and temperature (120–500 K) for measurements.

The measurement bridge used is shown in Fig. 2 [11]. It includes a data acquisition/control unit (HP3497A), a dc power supply (HP6625A), an integrating voltmeter (HP3458A) which provides integration from 0 to 16667 ms, an external trigger unit (HP3437A), and a C-MOS digital switch which is

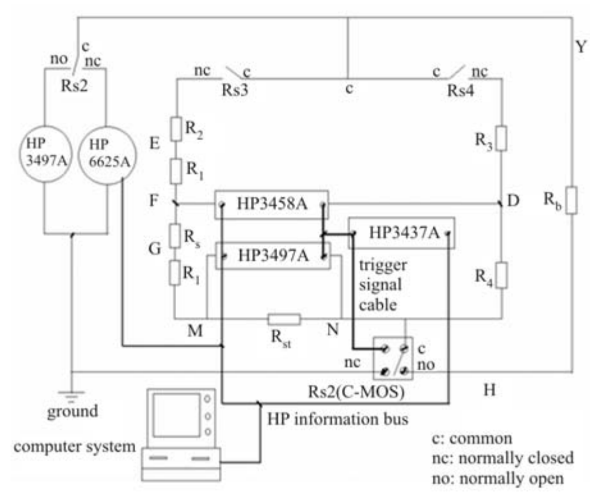

Fig. 2 Electrical system for measurement of thermal conductivity and thermal diffusivity

Table 1 Hot-wire specifications

Calibration equation: $R=a_0+a_1T+a_2T^2+bP$; T/°C, P/MPa		
Wire specifications and calibration coefficient		
material	platinum	platinum
purity/%	99.999	99.999
length/m	0.08549±0.00001	0.03395±0.00001
nominal diameter/μm	12.7	12.7
measured diameter/μm	13.06±1.1%	13.06±1.1%
a_0	62.22233	24.73335
a_1	0.248691	0.0976522
a_2	$-6.196378\cdot10^{-5}$	$-1.688681\cdot10^{-5}$
b	$-1.28134\cdot10^{-3}$	$-6.27643\cdot10^{-4}$

used to switch from the 'dummy' to the 'measurement' circuit. HP3497A is used to provide constant currents of 1, 0.1 and 0.01 mA when calibrating the wires and balancing the bridge, and also as an integrating voltmeter with integration times of 0.167, 1.67, and 16.67 ms along with digital switches used to monitor the circuit, under computer control, during the preliminary balancing as well as during the measurement process. HP6625A provides a high-stability fast response power supply with 0 to 16 VDC output to the hot-wire.

The hot-wire cell consists of two 12.7 μm nominal diameter platinum wires; a long wire 8.549 cm in length and a compensating short wire 3.395 cm long with resistances of approximately 62.2 and 24.7 Ω respectively at 0°C. Table 1 shows the wire specifications. These wires are connected to different arms of the four-arm bridge. The total resistance of each arm is adjusted close to 100 Ω with the ballast resistances R_1, R_2 R_3, R_4 and the 25 Ω standard resistance R_{std} (Fig. 2). As indicated above, the HP3497A Data Acquisition System is used for several purposes. First, it provides a voltmeter to measure the voltage across the standard resistance, R_{st}, to accurately determine the current through the hot-wires. Second, it also supplies 1 mA current used for balancing the bridge. Finally, it provides the digital switches for switching operations in the circuit. HP3458A is used to measure the transient imbalance of the bridge introduced by the temperature change of the hot wires and the voltages in every branch of the bridge. The methods of determining and correcting the bridge balance and the effective 'zero-time' residual bridge imbalance corrections are given elsewhere [10, 11].

Once all four arms the bridge are balanced with 1 mA current, the current is switched through the resistor R_b (Fig. 2) which is adjusted to the equivalent resistance of the four-arm bridge. The current through R_b is then increased in the range of 10 to 60 mA which, when switched through the bridge initiates a transient temperature rise in the hot-wires. The temperature rise of the hot-wire is limited to within 2 to 3°C in measurements with liquid *n*-pentane. The resulting change in the resistance of the hot-wires produces the transient imbalance of the bridge from which the precise ΔT_w∼time history of the hot-wire is determined for thermal properties measurement. The HP3437A is used to trigger HP3497A, HP3458A, and C-MOS switch to connect circuit components and to begin simultaneous measurements of both the current and the voltage across the bridge elements.

Results and discussion

For fluids which do not absorb thermal radiation, for example argon, the plot of ΔT∼ln$t$ is shown in Fig. 3 [1]. A similar behavior is observed with nitrogen. In these cases, a straight-line behavior is observed from the very beginning. The deviation plot resulting from a linear fit to ΔT∼ln$t$ data shows a random behavior without any definite trend. Figure 4 [1] shows the deviation plot for argon at 323 K and 20.9 MPa. For fluids which absorb thermal radiation, such as liquid *n*-pentane, the corresponding re-

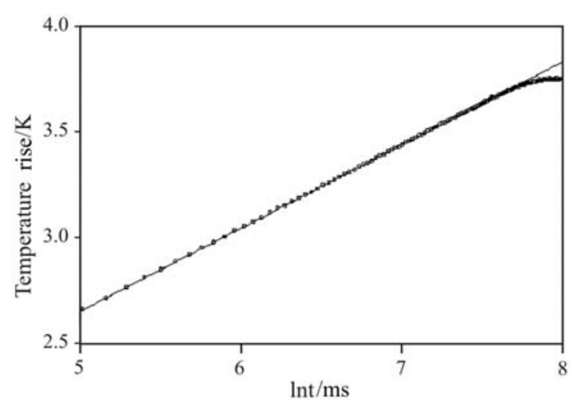

Fig. 3 Temperature rise ~ln$t$ for a measurement on argon at 323 K and 20.9 MPa

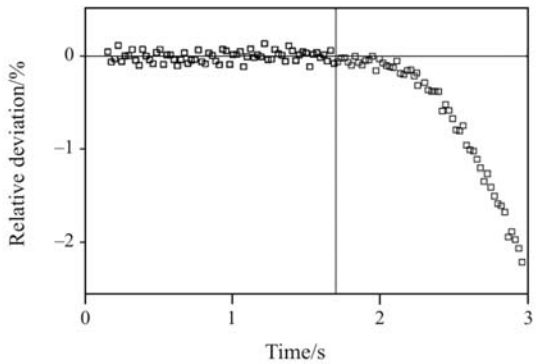

Fig. 4 Deviation in the thermal conductivity of argon at 323 K and 20.9 MPa from the linear fit

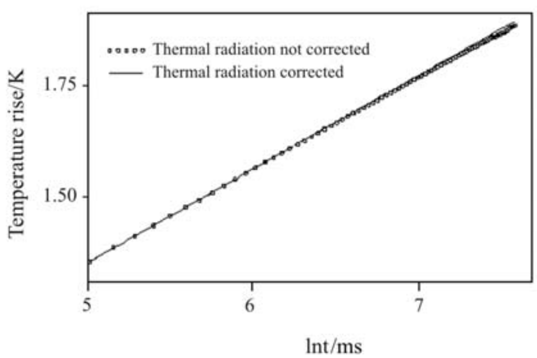

Fig. 5 Temperature rise as a function of ln*t* before and after fluid thermal radiation corrections: *n*-pentane at 376 K and 34.17 MPa and a power of 0.28036 W m^{-1}

sult is shown in Figs 5–7 [1]. A nearly straight line behavior of $\Delta T\sim\ln t$ data is observed. However, due to radiation effect, the straight line fit results in a deviation plot which shows a curvature effect. Figure 6 shows the deviation plot for uncorrected $\Delta T\sim\ln t$ data corrected for all non-ideal effects except for radiation effect. Figure 7 shows the deviation plot of $\Delta T\sim\ln t$ data for both uncorrected and corrected radiation effect data using Eq. (2.3) [1, 3, 11].

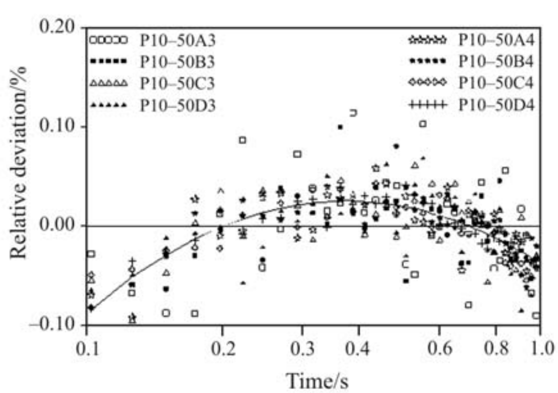

Fig. 6 Deviations of the corrected (aside from fluid radiation) temperature differences from the best-fit straight line for a series of *n*-pentane experiments near 376 K and 34.2 MPa

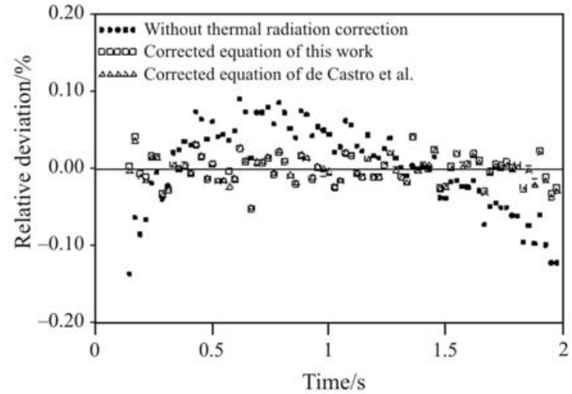

Fig. 7 Deviation of fluid radiation-uncorrected and radiation-corrected temperature rise from the linear fit: *n*-pentane at 376 K and 34.17 MPa with q=0.28036 W m^{-1}

The curvature observed with liquid *n*-pentane in Figs 6 and 7 is due to thermal radiation effect and not natural convection. This can be illustrated by comparing $\Delta T\sim\ln t$ response for argon and *n*-pentane. The commencement of free convection is detected by a departure from the straight line of the corrected temperature difference, $\Delta T\sim\ln t$ data provided it is remote from regions where outer boundary effects can be observed [5]. In Fig. 3 [1], measurement of corrected temperature difference over a 2 s period for argon at 323.56 K and 20.93 MPa (λ_o=0.02852 W $m^{-1}K^{-1}$, α_o=12.35·10^{-8} m^2 s^{-1} [10]) is shown. The deviation from a linear fit of the corrected temperature difference is indicated in Fig. 4 [1], where the departure from linearity after 1.7 s (Fig. 4) indicates the onset of convection. A comparison of these deviation plots (Figs 6 and 7) with that for argon (Fig. 4) clearly establishes that the curvature trend observed with *n*-pentane is due to radiation effects. Table 2 [10] for argon indicates that as the time frame for the determination of λ from the data set is extended and/or contracted from 0.12 to 1 s and then to 1.7 s, there is no significant (≤0.2%) difference in the value of λ returned. The modified Raleigh number, $Ra=g\beta\Delta T\delta^3/(\nu\alpha)$, for the commencement of convection for this measurement is 1.3·10^5, a value that compares favorably with the predicted 'critical' criterion $Ra\geq10^5$ based upon the conduction layer thickness at time *t* [13].

The exact determination of the influence of fluid thermal radiation requires consideration of the full

Table 2 Thermal conductivity of argon at 323.56 K and 20.93 MPa, q=0.13915 W m^{-1}

Time frame/s	λ/W m^{-1} K^{-1}	T_{ref}/K
0.12–1.00	0.02857	326.53
0.12–1.70	0.02852	326.63
1.00–1.70	0.02852	327.07

Table 3 Thermal conductivity of *n*-pentane before and after correction for fluid radiation effects for a series of experimental runs near 376 K and 34.2 MPa

TEST ID# Sun [11]	*T*/K	*P*/MPa	*q*/W m^{-1}	λ/W m^{-1} K^{-1} radiation uncorrected	λ/W m^{-1} K^{-1} radiation corrected	Difference radiation effect/%
P10_50A3	376.88	34.17	0.15803	0.1065	0.1049	1.53
P10_50B3	376.86	34.17	0.15802	0.1065	0.1047	1.62
P10_50C3	377.22	34.17	0.21478	0.1065	0.1049	1.53
P10_50D3	377.23	34.17	0.21500	0.1060	0.1048	1.15
P10_50A4	377.60	34.17	0.28036	0.1068	0.1048	1.91
P10_50B4	377.59	34.17	0.28029	0.1069	0.1049	1.91
P10_50C4	377.93	34.17	0.35441	0.1070	0.1048	2.10
P10_50D4	377.92	34.17	0.35452	0.1074	0.1048	2.48

form of the appropriate integral-differential energy equation. Its numerical solution is reported by Menashe *et al.* [9] for specified conditions and selected fluids in the *n*-alkane series. The deviation of the temperature rise of the hot wire was simulated for measurements in *n*-heptanes from the best-fit straight line. It is clearly indicated (Fig. 6 of [9]) that a curvature in $\Delta T\sim\ln t$ deviation plot may be expected in these fluids. A similar behavior is observed with *n*-pentane for a range of power levels (heat dissipation rate for the hot-wire into the surrounding test fluid) used in measurements. In this example, the corrected (aside from fluid radiation emission) $\Delta T\sim\ln t$ data indicates, from the start, a consistent departure from linearity for all times with a shape that corresponds, almost exactly, to that indicated by Menashe *et al.* [9]. However, in case of *n*-pentane [14] the same authors stated 'that the effects of radiation introduce no significant curvature to the experimental line'. If the correction for fluid radiation to the *n*-pentane data of Fig. 6 is applied, the goodness of fit, as expressed by the deviation plot (Fig. 7), improves substantially, and results in a radiation-corrected measurement of the thermal conductivity. Table 3 shows the effect of radiation in measurements for *n*-pentane at 376 K and 34.17 MPa.

The full correction method [9] is time-consuming and computationally intensive and could not be directly applied to the experimental procedure. Nieto de Castro [7] showed that an approximate correction procedure could be implemented to account for the fluid radiation emission characteristics, although, as indicated earlier, the inner boundary condition was inappropriate. The revision of their analysis results in a correction only slightly different as illustrated in Figs 5 and 6, where the uncorrected and fluid radiation-corrected temperature differences are shown as functions of time for *n*-pentane. In this example, the value of fluid radiation correction B necessary to restore linearity is 0.025 s^{-1}, an empirical value determined through the use of Eqs (2) (3). It should be noted that for the above measurement, *Ra* is only 8330 and there is no convection despite the extension of the measurement time to 2 s.

Radiation also influences the measurement of thermal diffusivity for two reasons. One is that the radiation effect can influence the temperature rise of the hot wire; therefore move the intercept of $\Delta T\sim\ln t$ line which always affects thermal diffusivity directly. The second is that radiation affects the conductivity values of the fluid which in turn influences the thermal diffusivity values (Eq. (7) of [1]).

Conclusions

Thermal radiation is one of the major correction terms for the difference between the actual and the ideal model in the transient hot wire technique to measure thermal conductivity and thermal diffusivity of fluids. It influences both, fluids which are transparent to thermal radiation and fluids which absorb thermal radiation. For thermal radiation absorbing fluids, the main part of this influence comes from radiation emitted from the absorbing fluids and not from their absorption. It is also necessary to distinguish between the influence of natural convection and radiation. Natural convection occurs only after the initial convection-free time has elapsed. This time is calculated by *Ra* number criterion after which curvature may appear in the deviation plot. For argon at 323 K and 20.9 MPa, this criterion gives a convection-free time of 1.7 s. But the radiation effects begin at the very beginning of the measurement process. Thus the curvature in the deviation plot can be observed from the very beginning. Our measurements with transient hot-wire technique for *n*-pentane which is a radiation absorbing fluid, indicates the presence of thermal radiation effect on the thermal conductivity.

Acknowledgements

The work was performed under a program of studies funded by the Natural Sciences and Engineering Research Council of Canada, under Grant no. A8859 and A5477.

References

1 L. Sun, J. E. S. Venart and R. C. Prasad, Int. J. Thermophys., 23 (2002) 391.
2 L. Sun and J. E. S. Venart, Int. J. Thermophys., 26 (2005) 1.
3 L. Sun, J. E. S. Venart and R. C. Prasad, Int. J. Thermophys., 23 (2002) 1487.
4 H. S. Carslaw and J. G. Jaeger, Conduction of Heat in Solids, Clarendon Press, 2nd Ed., Oxford 1959, p. 339.
5 J. J. Healy, J. J. de Groot and J. Kestin, Physica, 82C (1976) 393.
6 C. A. Nieto de Castro, R. A. Perkins and H. M. Roder, Int. J. Thermophys., 12 (1991) 985.
7 C. A. Nieto de Castro, S. F. Y. Li, G. C. Maitland and W. A. Wakeham, Int. J. Thermophys., 4 (1983) 344.
8 R. A. Perkins, H. M. Roder and C. A. Nieto de Castro, J. Res. Nat. Bur. Sds., 96 (1991) 247.
9 J. Menashe and W. A. Wakeham, Int. J. Heat Mass Transfer, 25 (1982) 661.
10 L. Sun, J. E. S. Venart and R. C. Prasad, Int. J. Thermophys., 23 (2002) 357.
11 L. Sun, Simultaneous Measurement of Thermal Conductivity and Thermal Diffusivity, Doctoral Dissertation, University of New Brunswick, Fredericton, NB, Canada 2001.
12 E. F. Buyukicer, J. E. S. Venart and R. C. Prasad, High Temperature–High Pressure, 18 (1986) 55.
13 G. H. Wang, J. E. S. Venart and R. C. Prasad, The Radiation Effect in the Transient Line-Source Technique for Thermal Properties Measurement, Proceedings of 11th Symposium on Thermophysical Properties, June 23–27, 1991, Boulder, Colorado, USA.
14 J. Menashe and W. A. Wakeham, Ber. Bunsen-Ges. Phys. Chem., 85 (1981) 340.

CTAS 2005
OnlineFirst: October 20, 2006

DOI: 10.1007/s10973-006-7711-2